Engineering Structures 56 (2013) 1820–1835

Contents lists available at ScienceDirect

Engineering Structures

journal homepage: www.elsevier.com/locate/engstruct

Development and testing of precast concrete beam-to-column connections

H.-K. Choi [a], Y.-C. Choi [b], C.-S. Choi [a,*]

[a] Hanyang University, Department of Architectural Engineering, 17 Haengdang-Dong, Seongdong-Gu, Seoul 133-791, Republic of Korea
[b] Chungwoon University, Department of Building Equipment and Fire Protection System, San 29 Namjang-ri Hongseong-gun, Chungnam 350-701, Republic of Korea

ARTICLE INFO

Article history:
Received 13 March 2012
Revised 3 July 2013
Accepted 17 July 2013
Available online 6 September 2013

Keywords:
Precast concrete
Beam-to-column
Connection
Steel plate connection
Engineered cementitious composite
Seismic performance

ABSTRACT

Five half-scale interior beam-column assemblies representing a portion of a frame subjected to simulated seismic loading were tested, including one monolithic specimen and four precast specimens. Variables included the detailing used at the joint to achieve a structural continuity of the beam reinforcement, and the type of special reinforcement in the connection (whether ECC or transverse reinforcement). The specimen design followed the strong-column-weak-beam concept.

The beam reinforcement was purposely designed and detailed to develop plastic hinges at the beam and to impose large inelastic shear force demands into the joint. The joint performance was evaluated on the basis of connection strength, stiffness, energy dissipation, and drift capacity. From the test results, the plastic hinges at the beam controlled the specimen failure. In general, the performance of the beam-to-column connections was satisfactory. The joint strength was 1.15 times of that expected for monolithic reinforced concrete construction. The specimen behavior was ductile due to tensile deformability by ECC and the yielding steel plate, while the strength was nearly constant up to a drift of 3.5%.

1. Introduction

Precast concrete members have various advantages in service and quality in comparison with cast-in-place concrete ones: better allowance for quality control, ready supply of good quality aggregates, and much higher strength due to better batching and quality control of concrete through the use of a specialized labor force under factory conditions. However, the joints between the prefabricated members have some issues. Joints can be considered as the weakest and the most critical parts of a precast concrete structure. Precast concrete frame construction is not used extensively in high-seismic regions of most countries [1–4]. Connections, in particular beam-to-column connections, are the vital part of precast concrete construction. To satisfy the structural requirements of the overall frame, each connection must have the ability to transfer vertical shear, transverse horizontal shear, axial tension and compression, and occasionally bending moment and torsion between one precast component and another, safely. The transfer of forces between the components and eventually the behavior of frames are governed by the characteristics of the connections. However, in practice, the behavior of precast connections is not well established and not fully understood to fulfill the requirements needed in the design and construction development of precast technology.

Precast reinforced concrete systems with cast-in-place concrete are joints designed to behave as a cast-in-place reinforced concrete structure which have been used in the construction of earthquake resisting multistory buildings. Since precast reinforced concrete system was substantially unreasonable and had many uncertainties against the earthquake loading, these precast concrete systems are designed to have appropriate levels of strength, stiffness, ductility and energy dissipation characteristics at least equal to those of an equivalent conventional reinforced concrete (RC) system. This made a precast system could not be used in wide area of construction sites [5]. As recognized, the challenge in precast frame constructions lies in finding economical and practical methods of connecting the precast concrete elements together to ensure adequate stiffness, strength, ductility, and stability. A number of experimental research programs conducted in recent years have significantly improved our understanding of the behavior of connections between precast concrete elements [6]. For example, internal resisting mechanisms have been identified and understood and design and detailing requirements have been developed [7–10]. In some research programs, precast elements have been connected at the beam-to-column joint region; in others, elements have been connected at mid-span (in the case of beams) and at mid-height (in the case of columns). Since one advantage of using one-way perimeter frames is the reduced complexity of the design and construction of the beam-to-column joints, many studies have focused on the performance of perimeter precast concrete frame joints [1–10].

In emulation systems, precast beam longitudinal reinforcement that is connected at a beam-to-column joint is commonly spliced.

* Corresponding author. Tel.: +82 2 2220 2371.
E-mail address: ccs5530@hanyang.ac.kr (C.-S. Choi).

0141-0296/$ - see front matter © 2013 Elsevier Ltd. All rights reserved.
http://dx.doi.org/10.1016/j.engstruct.2013.07.021

Splicing can be achieved through proprietary steel sleeves or by lap splicing bars, which may be bent to form 90° standard hooks. In other cases, continuity at the joint has been achieved by means of bonded post-tensioning, ungrouted post-tensioning, or mild reinforcing steel bars grouted inside the joint but with an unbonded length adjacent to the column face [6–10].

This paper reports the behavior of concrete frames under cyclic loading of a precast concrete beam-to-column connection developed and used in South Korea. In the frame under consideration, design and detailing were aimed at emulating monolithic construction, as is required in the ACI-ASCE [11] and ACI 318-05 [12]. The principal objective of this research program was to develop a ductile moment-resisting connection for precast reinforced concrete frames capable of resisting seismic loading. This investigation was conducted to assess the joint behavior and its stiffness, deformation, and strength characteristics when subjected to large shear and bond force demands.

2. Research significance

Based on experimental study on half scale connections, the objective of the research program was to further develop the formation of safe and economical ductile precast reinforced structures meeting the building code requirements. This study present experimental data that show the seismic performance of the beam-column connection developed is as good as or better than similar conventional cast-in-place connection. Their utilization saved construction time and cost, insured better quality control, and suggested the achievement of standardization.

3. Literature review

3.1. Conventional connection

In recent years, several studies have been conducted on the behavior of precast beam-to-column connections designed to resist earthquake loading. Major problems were related to the low energy dissipation capacity of precast members and the strength demand on connections, i.e., the ability of the structures to undergo large inelastic deformations without substantial loss of strength.

Many types of beam-column connections have been developed to join precast beam elements to column elements. About 25 typical precast beam-column connection details recommended by the Prestressed Concrete Institute (PCI) were based on simplicity, durability, and construction tolerance rather than on strength and stiffness. Consequently, all of these details exhibited one or more of the following disadvantages: slow erection, no reliable moment capacity, construction tolerance problem, and expensive connection hardware.

Prestressed and hybrid connection details are major ductile connections minimizing the damage to the joint. However, the necessity to lay duct to install tendon penetrating a beam-to-column joint makes their construction complicated and additional equipment and technology are needed to introduce prestressing [13–14]. Dywidag Ductile Connection (DDC) method, in which ductile load is inserted to columns, beam and column are bolted, and thus all structural connections can be completed, is one of the commercialized connection details featuring excellent ductility. However, it has drawbacks such as the high cost of ductile load and high precision required in construction [15–17].

In 1993, Soubra [18] suggested a new connection detail for the precast column-to-beam connection which featured installing U-shaped steel bars to precast beams and columns, uniting the steel bars, and casting fiber-reinforced concrete (FRC) to the joint in the field. The experimental study conducted for evaluating the seismic performance of outside type connections showed that the fiber improved seismic performance significantly. However, the connection had disadvantages associated with assembling U-shaped steel bars and casting FRC. Alcocer [2] developed a new connection detail in which hoops were used to confine the hook of the lower steel bars of precast columns. The evaluation of seismic performance of the detail showed that the strength, stiffness, and deformation required upon the design of joints were secured. However, a multiple number of steel bars should be installed in relatively narrow joint core and fabricating steel bars was complicated. In order to improve the constructability of a connection, Khaloo [19] developed a connection detail where connectors were used to connect lower steel bars of half precast beam at the joint face instead of connecting them in the precast beam-to-column joint. It was reported that the capacity of the joint was influenced by axial load and the horizontal reinforcement installed within the connection length considerably affected deformation capacity. While studies found the details excellent in seismic performance, their field application is not considered fairly feasible.

3.2. Development connection

The new connection detail suggested in this study is characterized by ductile connection, steel connectors, and engineered cementitious composite (ECC) which is a kind of high performance fiber reinforced cement composite with multiple fine cracks (HPFRCCs) and used in order to improve the constructability of joint and efficiently transfer stress between discontinued precast members. Making steel connector consists of bolting steel tubes and steel plates which are usually placed inside the precast column and beam and casting the ECC to some parts of the beam and joint in the field (refer to Figs. 1 and 2).

The connection detail has advantages such as simple connection by metal and excellent constructability. In addition, 1% of fiber volume fraction in the ECC cast to the joint improves tensile deformability by 3–4% when compared with nominal concrete. It provides enough toughness against shear stress caused by horizontal loads such as an earthquake and thus improves the seismic performance of the joint. Securing flowability is indispensable in the ECC suggested in this study. Therefore, self-compacting ECC was developed through the variation of fiber types and volume fractions [20–21]. Moreover, two types of beam-column connection are developed in this study: one is to connect beams and columns at a certain distance (0.3d; d *is beam widths*) from the column face (outside type shown in Fig. 3) and the other is to join beams and columns at the column face (inside type illustrated in Fig. 3). In case of the outside type, a plastic hinge was designed to occur at the outside of the connection part by securing a distance (0.3d) from the column face and workability was expected to improve through easier member lifting. The connection detail avoids mutual interruptions between steel bars crossing each other at the joint and can be easily produced in a factory because the lower steel bars at precast beams do not protrude outside. The fabrication process is as follows: (1) After a precast column is set up, a precast beam is assembled and bolted to a column steel connector; (2) Slabs are installed by the same steel connector or deck slab; (3) Initial prestress is applied to the bolts to improve the stiffness and seismic performance of the joint; and (4) the ECC is cast to each joint.

4. Specimen design and test procedure

4.1. Specimen design

In order to evaluate the seismic performance of the precast beam-column connection developed in this study, beam-to-column

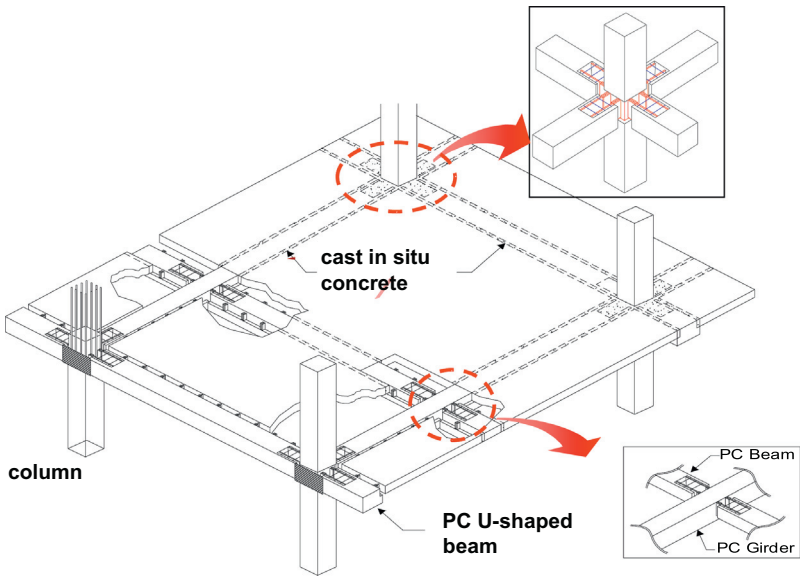

Fig. 1. Description of system concept.

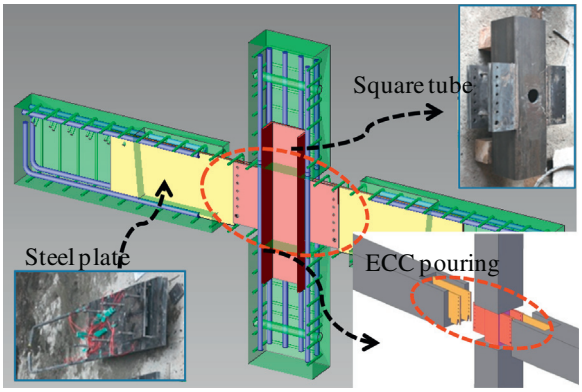

Fig. 2. Description of development precast concrete beam-to-column connection.

specimens from interior connection were planned with variables such as in situ ECC area in the U-shaped beam and column joint, beam-column strength ratio, existence of lateral reinforcing bars, and connection detail.

The in situ ECC area in the beam was decided to range between 0.7*d* (250 mm) and 1.4*d* (500 mm) based on 1.0*d*, the distance of plastic hinge movement suggested in the previous studies [22,23], since plastic hinge at the beam-to-column joint face can be diffused to the inside of the beam due to the high tensile deformability of the ECC.

In general, design seismic load can be significantly reduced by allowing nonlinear behavior of structures when it comes to seismic design of structures. To secure the ductile behavior of a structure, enough displacement capacity of each member needs to be obtained and plastic hinges should be evenly distributed throughout the height of a structure. For the purpose of this, the flexural yielding of columns needs to be delayed by increasing the load-carrying capacity of columns and the ductility and energy dissipation capacity of a structure needs to be improved by evenly distributing nonlinear deformation to beams at each story, which strategy is typically used as strong column-weak beam design concept. To satisfy this concept, ACI 318-05 [10] and KCI [11] state that the summation of flexural strength of upper and lower columns should be 1.2 times larger than that of both side beams to avoid the premature collapse of columns in the special moment resisting frame system. In addition, ACI-ASCE 352 [12] suggests 1.4 times in strong seismic zones.

Linear analysis of a moment resisting frame system indicates that the upper and lower columns at a connection show two different bending moment distributions. However, according to existing research results [24,25], the moment distribution of a real moment resisting frame showing nonlinear behavior is different from that of an ideal portal frame, which results in high possibility of the flexural yielding of columns even though a structure is designed with the strong column-weak beam concept. Therefore, Bracci and Dooley [25] investigated the behavior of RC frame systems from the standpoint of possibility of exceeding the life safety limit state and reported that column-to-beam strength ratio should be

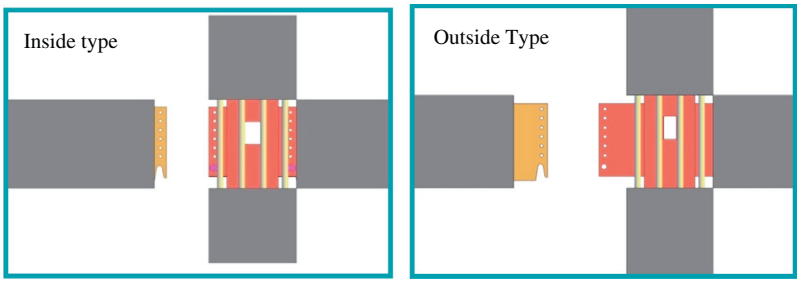

Fig. 3. Proposed connection type.

larger than 2.0. In general, if flexural strength ratio is relatively larger than 1.0, a plastic hinge forms at a beam. However, in this case, most damages are concentrated at a beam-column connection. If flexural strength ratio is much larger than 1.0, critical damages occur in a beam part slightly away from the connection. The capacity of the beam-column connection increases with the flexural strength ratio ranging from 1.0 to 1.9 [24–26].

As mentioned above, flexural strength ratio affects the connection capacity. Therefore, the effect of flexural strength ratio on the connection details developed in this study was evaluated. The control specimen was designed to have a flexural strength ratio of 1.6 which falls in the range suggested by the code [11,12]. A flexural strength ratio of 1.3 which is smaller than that of the control specimen was designed for the PC specimens. The failure mechanism at the connection and behavior of the PC specimens with the smaller flexural strength ratio were investigated through the design. In addition, the aforementioned two connection types were designed to assess the influence of connection types on the performance of PC specimens: outside and inside types.

The specimens represented a half-scale beam-column joint from the bottom story of a prototype office structure. The basic structural system for this building was a perimeter moment-resisting frame. The prototype building was rectangular, 15 stories high, and had plan dimensions of 24 × 30 m. The dimension of all the precast columns was 350 × 350 mm and □-200 × 200 × 12 commercial shape steel was used as the steel tubes inserted to the precast columns. The connection with the beam was welded on both sides. The dimension of the beams was 350 × 400 mm and PL-334 × 748(690) × 12 was used as the steel plates inserted to the precast beams. The nominal compressive strength of the concrete was 27 MPa and SD40 was used as steel connector and bars. The fastening strength of bolts improved the stiffness of the connection.

The ACI 318-05 [12] standard categorizes the design of RC beam-to-column joint under seismic loading into non-seismic region (Type 1) and seismic region (Type 2). As part of a column, a beam-column joint is substantially crucial since the joint failure can cause quite serious damages to a structure. Therefore, the capacity of a beam-column connection should be larger than that of a beam for a plastic hinge to occur in the beam until the design ductility criterion of a beam-column connection is met. To satisfy this, through comparison between the design strength of columns and the excess strength of beams (by considering strain hardening of steel reinforcement), columns are designed for plastic hinges not to occur in the columns (referring to the current design flexural strength ratio [11,12]). However, the capacity of a beam-column joint sometimes decreases due to a plastic hinge in a beam and thus the connection can be failed before the design ductility criterion is met. This is attributed to the phenomenon that the height of neutral axis of a beam section decreases and residual deformation increases when a plastic hinge forms due to yielding of main tension reinforcement in a beam close to a joint. In this case, strain increase of the main tension rebar in the beam penetrating the joint influences increase of diagonal crack width in the concrete compression region of the connection and thus the behavior of the joint can be changed. Therefore, the flexural strength ratio was computed by considering the yielding point of main tension rebar in the beam in this study.

Accordingly, all the specimens were planned to go through joint failure after beam yield and the load-carrying capacity. The joint shear strength (V_j) was calculated by Eq. (1) (ACI 352R-02) by multiplying the effective joint sectional area. In the equation, the shear strength factor, γ is 1.660 for Type 1 and 1.245 for Type 2.

$$v_j = \gamma \times \sqrt{f'_c} b_j \times h_c \quad (1)$$

The joint shear strength when the beam bar yields (v_{jby}) can be calculated as follows;

$$v_{jby} = \left(\frac{l_c}{z} - 1\right) v_{by} \frac{l_b}{l_c} - \frac{h_c}{z} v_{by} \quad (2)$$

where l_c is the column height, h_c is the joint height, z is the distance between the centroid of upper and lower beam bars and v_{jby} is the beam shear strength when the beam bar yields. As shown in Table 1, v_{j2}/v_{jby} value is over 1.0 in all of the specimens [27], which means that the specimens can fail after the yield of main tensile bars in the beams and satisfy the requirement of the ACI 352R-02 [11]

Table 1
Details of test specimen and material properties.

Specimens	Connection method	Hoop bar of Joint area	ECC area (mm)	Column size (mm)	Beam size (mm)	Column						
						Reinforcing bar (Upper and lower each)			Hoop			
						f_{cy} (MPa)	ρ_c	n_c	f_{hy} (MPa)	ρ_h	s_h (mm)	n_b
RC-Control	Cast-in-place	O	-	350 × 350	350 × 400	508	0.038	12-D22	475	0.011	50	D13
PC-OH-50	Outside connection	O	500(1.4d)									
PC-OH-25	Outside connection	O	250(0.7d)									
PC-IH-50	Inside connection	O	500(1.4d)									
PC-I-25	Inside connection	X	250(0.7d)									

Specimens	Beam							f'_c (MPa)		$\frac{\sum M_c}{\sum M_b}$	v_{j1} (kN)	v_{j2} (kN)	v_{jby} (kN)	v_{j1}/v_{jby}	v_{j2}/v_{jby}
	Reinforcing bar (Upper and lower each)			Stirrup				PC member	ECC member						
	f_{by} (MPa)	ρ_{bu}, ρ_{bl}	n_b	f_{sy} (MPa)	ρ_s	s_b (mm)	n_s								
RC-Control	437	0.012	8-D16	475	0.014	100	D13	27.5	-	1.6	1056	792	629	1.68	1.26
PC-OH-50	461	0.016	8-D19					27.5	40.5	1.3	1286	965	886	1.45	1.09
PC-OH-25	461	0.016								1.3	1286	965	886	1.45	1.09
PC-IH-50	437	0.012	8-D16							1.6	1286	965	629	2.05	1.54
PC-I-25	437	0.012								1.6	1286	965	629	2.05	1.54

f_{cy}; f_{hy}; f_{by}; f_{sy}: yield strength column bar, hoop, beam bar, beam stirrup respectively; ρ_c; ρ_h; ρ_{bu},ρ_{bl}; ρ_s: ratio of column bar; hoop, upper beam bar and lower beam bar, stirrup respectively; n_c; n_h; n_b; n_s: size of column bar, hoop, beam bar, stirrup respectively; f'_c: compressive strength of concrete and ECC; v_{j1}; v_{j2}: type 1 and type 2 shear strength of joint predicted by ACI 318-05, v_{jby}: joint shear strength when beam bar yields.

for Type 2. The dimensions and details of reinforcements of the specimens are shown in Figs. 2–8 and the other experimental parameters are listed in Table 1.

4.2. Test procedure

In this study, cyclic load test was carried out to evaluate the seismic performance of the inside joints of the half-scale specimens. The specimens were pinned at the column base and roller supported at the beam ends and column top as illustrated in Fig. 9. These boundary conditions were chosen to model actual conditions where the moments are approximately zero at mid-span of the beam and the column. Each specimen was first loaded axially to the level of $0.1f'_cA_g$ (Axial force applied to the specimen was computed to be approximately 10% of the product of compressive strength and sectional area of the column based on the result from a simple elastic analysis reflecting the dead and live loads of the prototype structure.) The top column displacements were recorded in each direction. The vertical and lateral loads were applied as shown in Fig. 9. Cyclic load was applied by a 1000 kN actuator connected to the top part of the column. The yield displacement, δ_y, was defined as the average of the two column displacements divided by 0.75. Although this displacement is the displacement of the top of the column, it corresponds to yielding in the beam. Fig. 10 depicts the test setup and the test facility. The ACI T1.1-01 [28] seismic test guideline for moment frames was used as loading protocol and load control up to 10% of yield load was followed by displacement control.

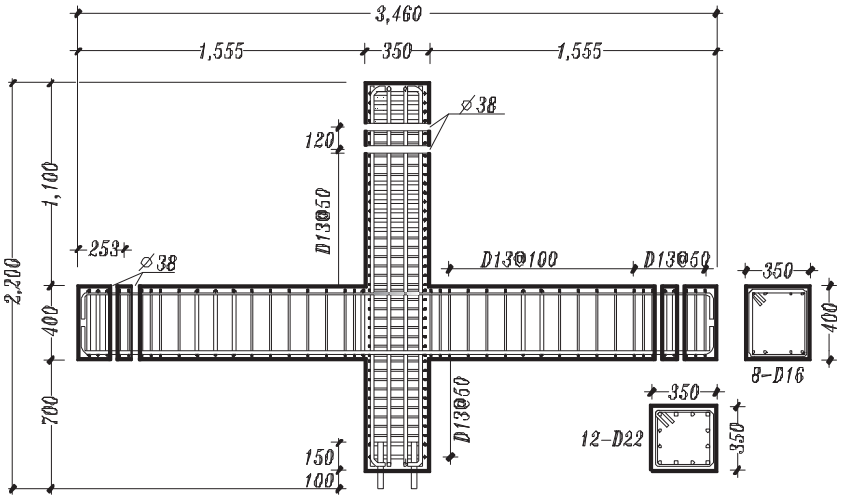

Fig. 4. Details of control specimen (RC) (Unit: mm).

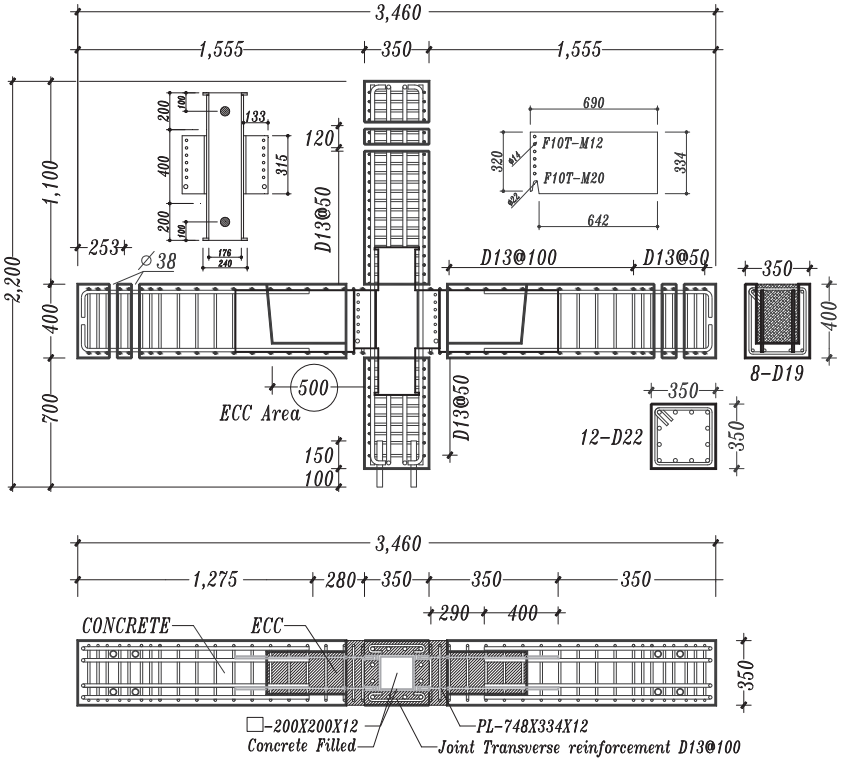

Fig. 5. Details of PC-OH-50 Specimen (Unit: mm).

5. Test results

5.1. Failure mode

The crack patterns of each specimen at failure are shown in Figs. 11–15. In general, the initial cracks formed at the beam-column interface and the flexural cracks propagated transversely in beams and extended longitudinally away from the column face with very similar crack spacings. Most of the flexural cracks in the beams were perpendicular to the axis of the members. Cracks initially occurred at the beam-to-column joint face and vertical flexural cracks with the similar spacing to each other propagated to the right and left ends.

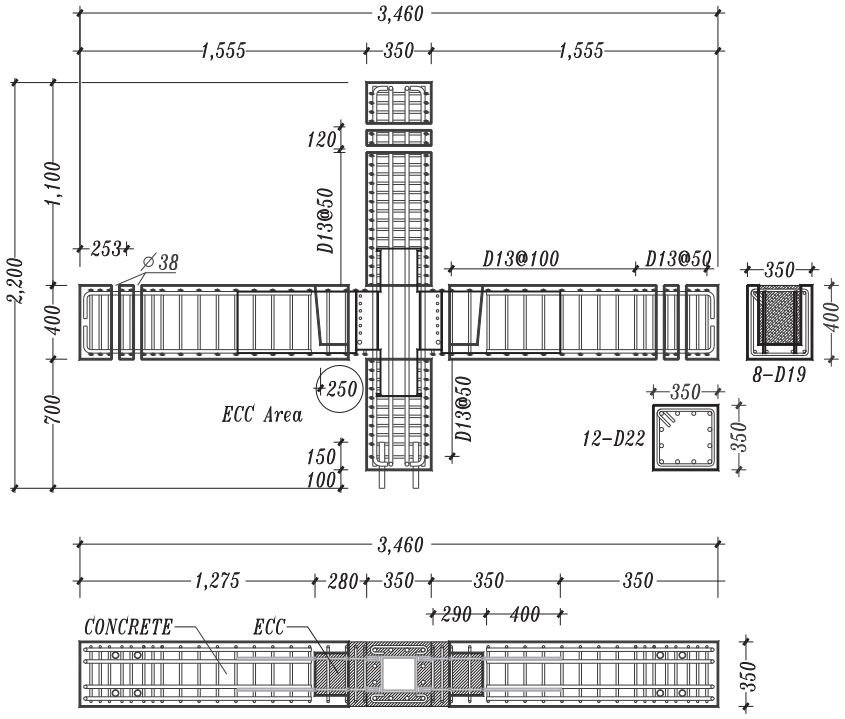

Fig. 6. Details of PC-OH-25 Specimen (Unit: mm).

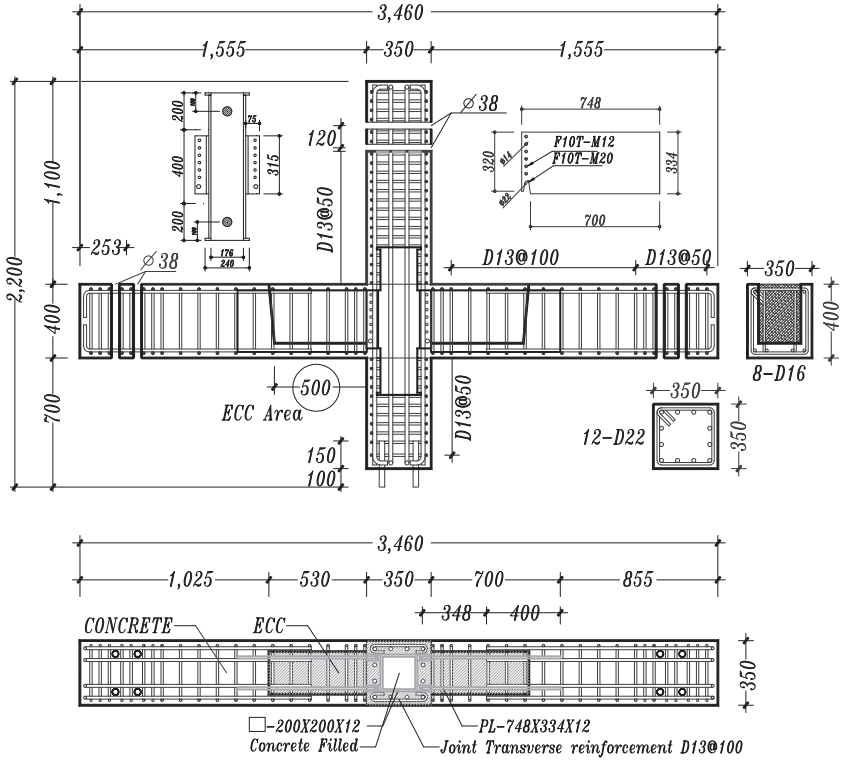

Fig. 7. Details of PC-IH-50 Specimen (Unit: mm).

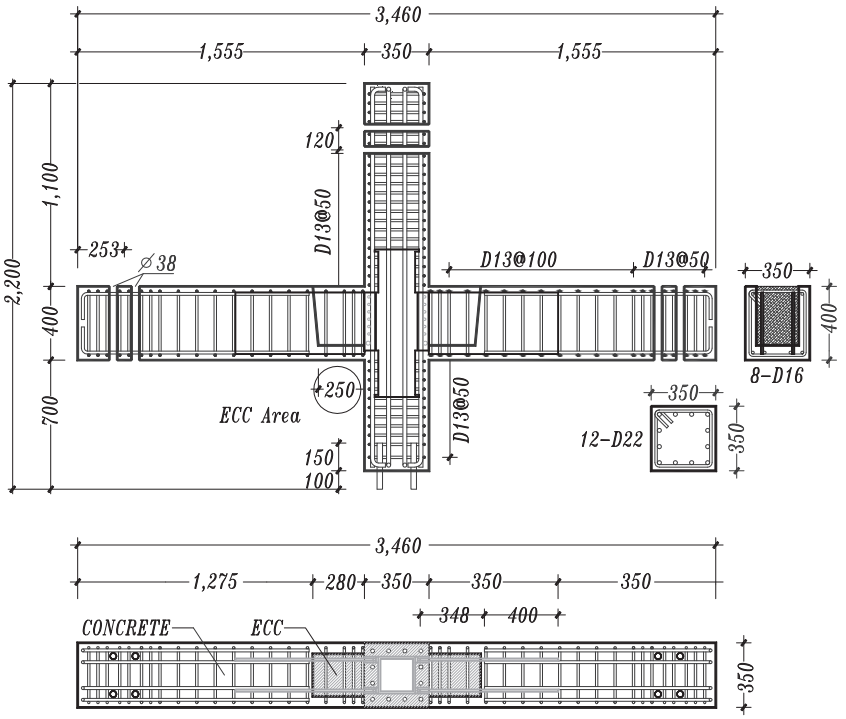

Fig. 8. Details of PC-I-25 Specimen (Unit: mm).

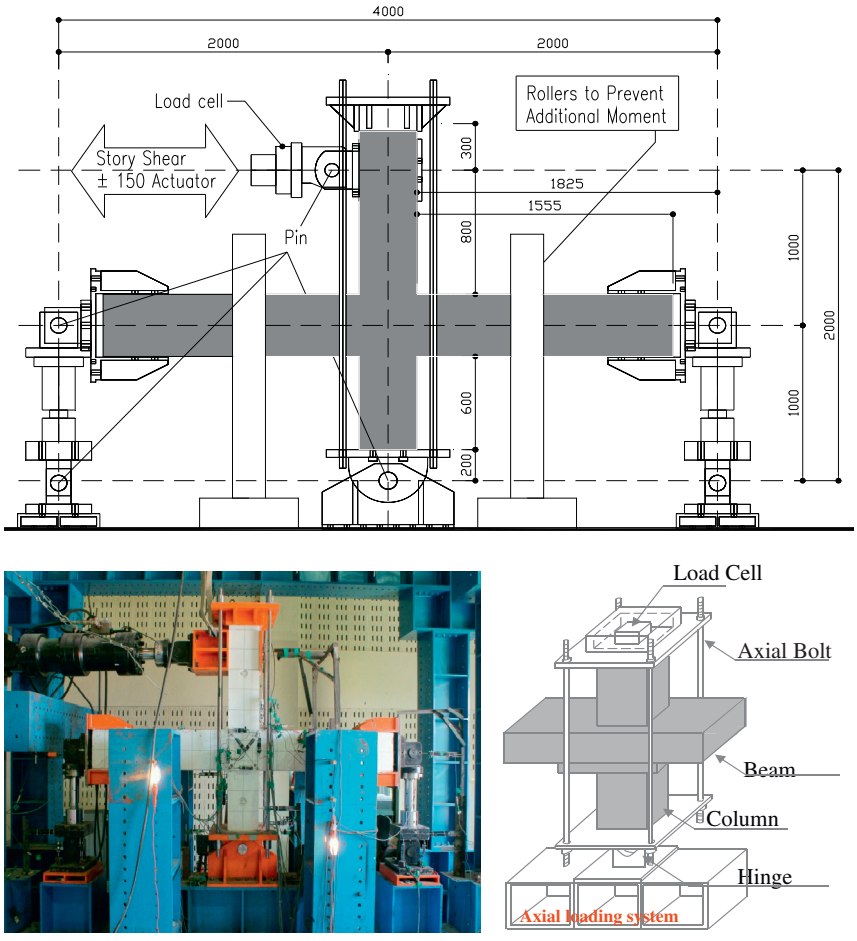

Fig. 9. Test Set-up.

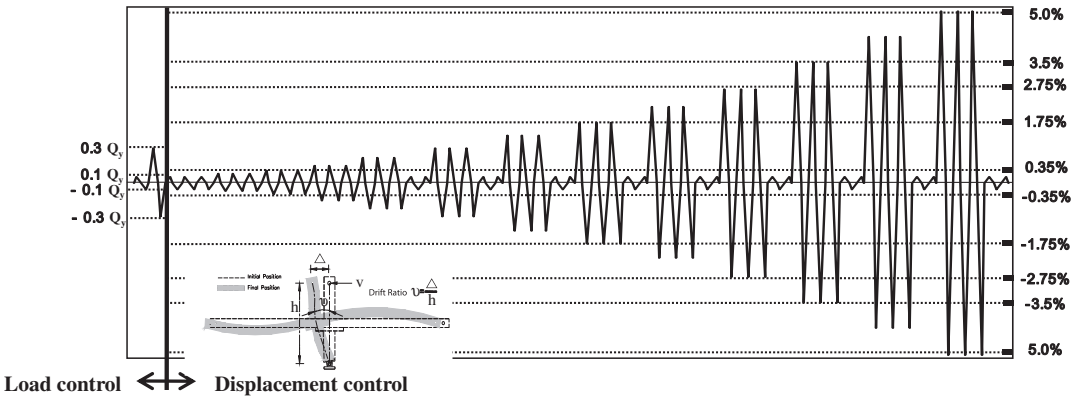

Fig. 10. Loading protocol.

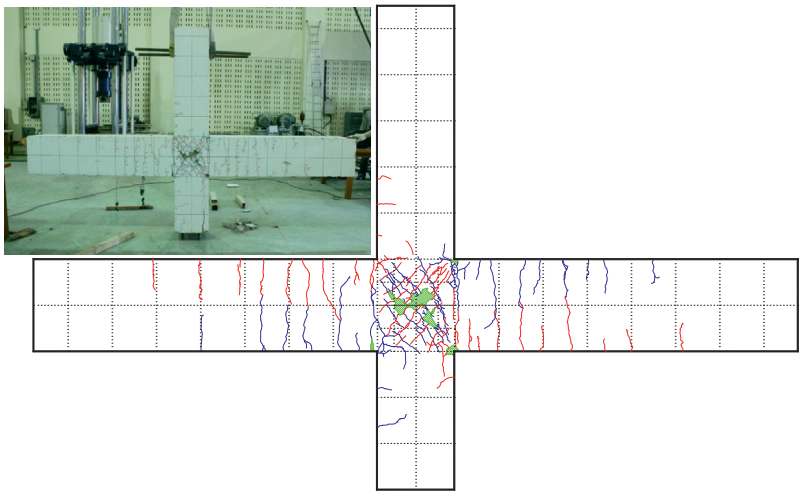

Fig. 11. Crack Patterns at Failure of RC-control specimen.

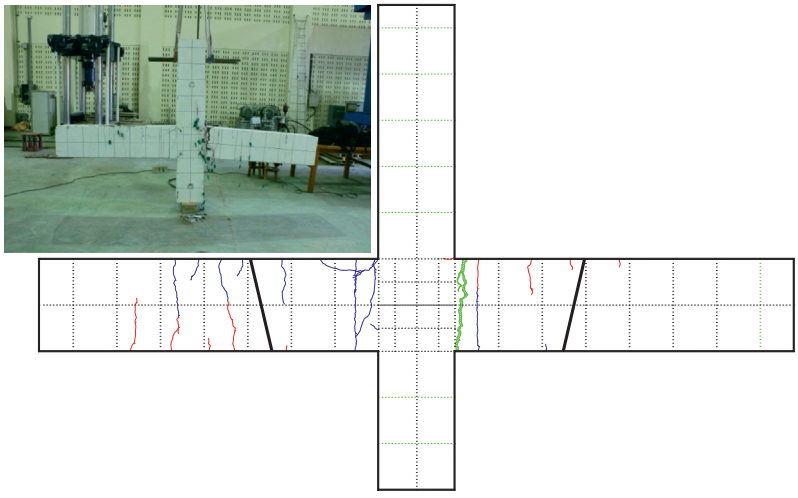

Fig. 12. Crack Patterns at Failure of PC-OH-50 Specimen.

(1) *RC-Control*: At a drift ratio of 0.2%, initial flexural cracks formed at both the beams and additional cracks occurred near the supports with increase of load. The initial cracks propagated at a drift ratio of 0.25%. Then, concrete spalling was observed at the joint when a drift ratio was 2.2%. Finally, the specimen failed due to crushing of the joint at a draft ratio of 3.5% (Fig. 11).

(2) *PC-OH-50 and PC-OH-25*: The two outside type specimens PC-OH-50 and PC-OH-25 had the ECC area of 500 and 250 mm, respectively. They showed quite similar behavior and failure mode to each other. Initial cracks were found at the interface between the joint face and the end of the ECC part at a drift ratio of 0.2% and additional cracks formed on the top of the beams as load increased. At a drift ratio of

0.5%, flexural cracks in the beam occurred at the end of the steel plate (700 mm from the joint face) and then existing cracks widened and propagated toward the supports. As a drift ratio increased, more hairline cracks were observed. However, the size of the cracks did not increase. When a drift ratio was 3.5%, concrete crushing occurred near the plastic hinge of the beams, resulting in the failure of the specimens (Figs. 12 and 13).

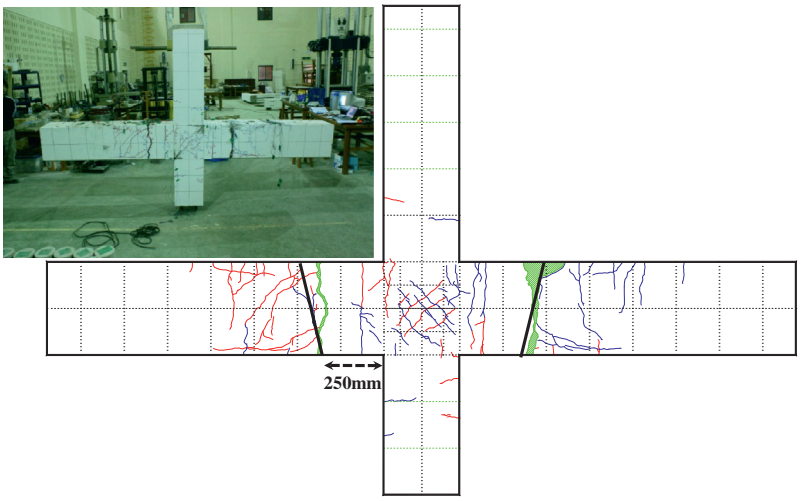

Fig. 13. Crack Patterns at Failure of PC-OH-25 Specimen.

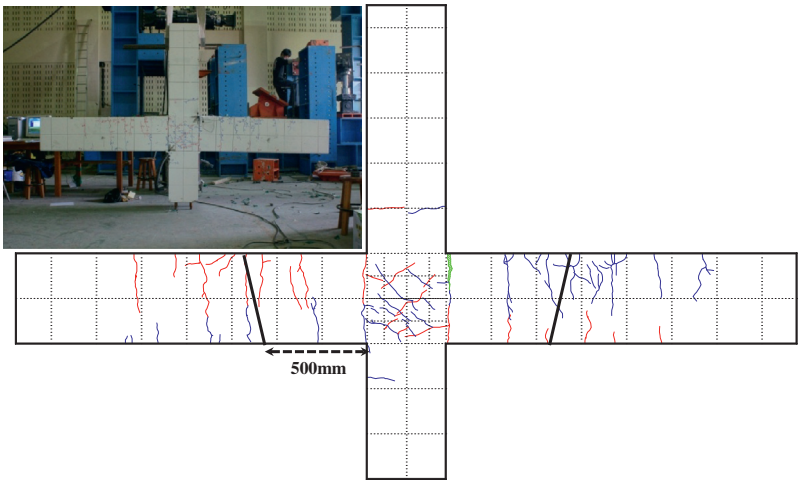

Fig. 14. Crack Patterns at Failure of PC-IH-50 Specimen.

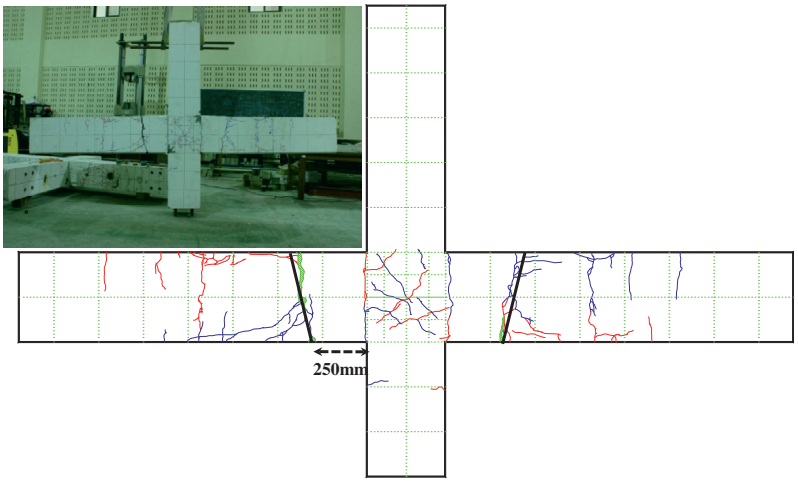

Fig. 15. Crack Patterns at Failure of PC-I-25 Specimen.

(3) *PC-IH-50 and PC-I-25*: The ECC areas were 500 and 250 mm for the inside type specimens PC-IH-50 and PC-I-25, respectively. The failure modes of the inside type specimens were similar to that of PC-OH-50. However, in case of PC-I-25 without hoop reinforcement in the connection, after the initial crack formation, flexural cracks in the beam were found at the end of the steel plate (700 mm from the connection face) at a drift ratio of 0.25%. This difference was probably attributed to the fact that the area of the ECC poured into the plastic hinge region of the beam was small. Moreover, the difference was probably due to no hoop reinforcement in the joint (Fig. 14 and 15).

In case of the RC specimen with column to beam strength ratio of 1.6, the beam yield preceded the column yield. Thus, the beam moment was redistributed to the column and cracks were evenly distributed along the shear plane of the beam. Then, diagonal shear cracks at the joint core were followed by final failure. Unlike the RC specimen, the PC specimens exhibited different behaviors depending on the connection type and flexural strength ratio. In case of PC-OH-50 with in situ ECC area of 500 mm in which the beam-to-column connection was at a distance of 0.3*d* from the column face, a plastic hinge developed at the connection between the members (0.3*d*) and cracks concentrated in the plastic hinge after yield load. It was delivered to the joint and the width of the cracks increased along with hairline cracks. On the contrary, PC-OH-25 with in situ ECC area of 250 mm, a plastic hinge developed at the connection face and extended beyond in situ ECC area (1.4*d*) and cracks spreading over the beam shear plane were followed by final failure. As for PC-IH-50, while a plastic hinge developed around 0.3*d* and cracks spread to the support, joint failure was not observed. On the other hand, in case of PC-I-25 which did not have hoop bars inside the joint area and had small in situ ECC area, a plastic hinge developed at 1.4*d* and multiple diagonal shear cracks were observed at the joint. Based on the observation of the cracks, in the connection details suggested in this study, the steel connector and in situ ECC area could induce a certain length of plastic hinge and in situ ECC area of 0.7*d* (250 mm) is efficient for reinforcing the area of plastic hinge regardless of variables.

5.2. Load–displacement

Fig. 16 illustrates the load–drift ratio curves of the test specimens subjected to cyclic loading, where displacements were

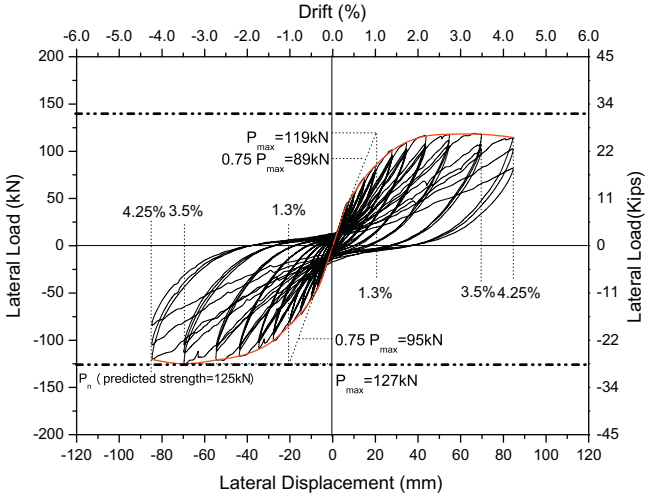

Fig. 16. Load-Drift Ratio of RC-Control Specimens.

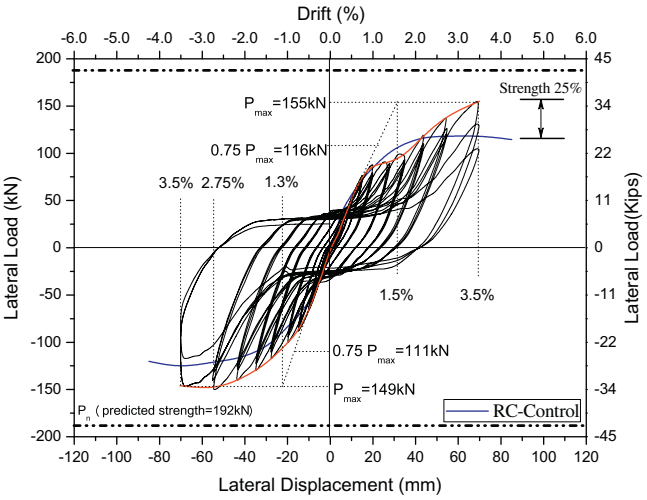

Fig. 17. Load-Drift Ratio of PC-OH-50 Specimens.

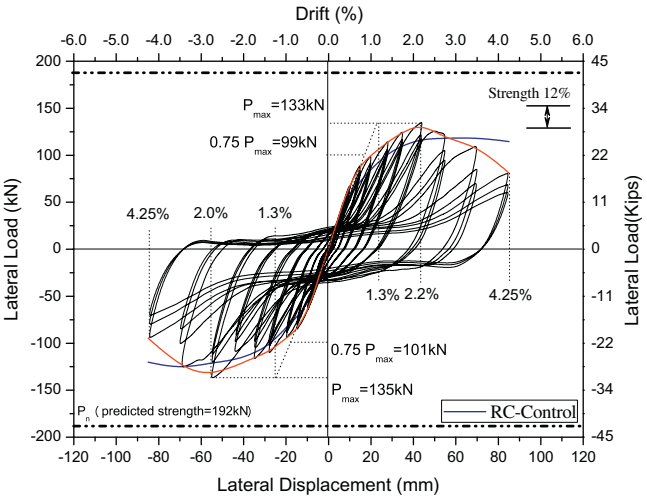

Fig. 18. Load-Drift Ratio of PC-OH-25 Specimens.

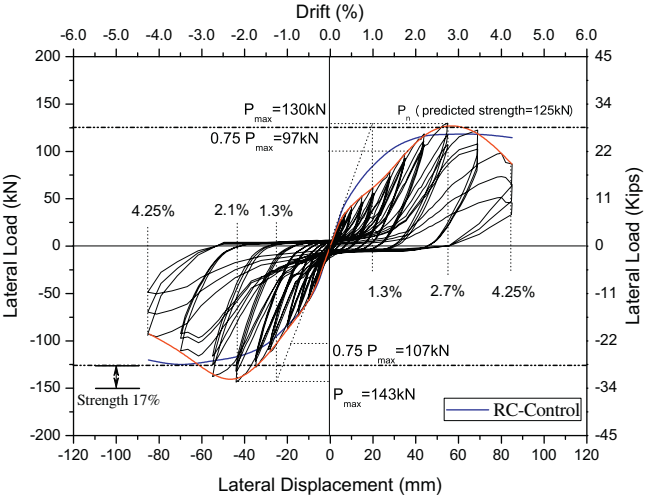

Fig. 19. Load-Drift Ratio of PC-IH-50 Specimens.

Table 2
Test results.

Specimen		P_y (kN)	P_{max} (kN)	P_f (kN)	δ_y (%)	δ_{max} (%)	δ_f (%)	u (−)	M_n (kN m)	M_{uj} (kN m)	M_{peak} (kN m)	v_n (kN)	v_u (kN)	v_{peak} (kN m)	$\frac{v_{peak}}{v_u}$
RC-control	Pos	89	119	114	1.5	3.5	4.25	2.3	125	285	206	792	540	572	1.06
	Neg	95	127	120	1.9	3.5	4.25	1.8			219			611	1.13
PC-OH-50	Pos	116	155	100	1.6	3.5	3.5	2.2	192	345	267	965	901	746	0.83
	Neg	112	149	110	1.3	2.75	3.5	2.6			256			717	0.8
PC-OH-25	Pos	99	133	77	1.2	2.20	4.25	1.8	192	345	229	965	901	640	0.71
	Neg	101	135	90	1.25	2.75	4.25	2.2			232			649	0.72
PC-IH-50	Pos	97	130	86	1.4	2.75	4.25	2.1	125	346	225	965	540	625	1.17
	Neg	107	143	92	1.25	2.75	4.25	2.2			125			688	1.27
PC-I-25	Pos	103	138	119	1.7	2.2	3.5	1.3	125	346	238	965	540	664	1.23
	Neg	90	121	112	1.3	2.75	3.5	2.1			125			582	1.08

All estimates associated with moment and shear computed based on actual material properties. P_y: moment at first yield of top bar (measured), P_{max}: peak load(measured), P_f: failure load(measured), δ_y: yield displacement (measured), δ_{max}: peak displacement(measured), δ_f: failure displacement(measured), u: ductility(δ_{max}/δ_y), M_n: nominal moment, M_{uj}: moment corresponding to v_n (computed), M_{peak}: peak moment(measured), v_n: nominal joint shear capacity(computed), v_u: joint shear demand(computed), v_{peak}: joint shear at M_{peak}.

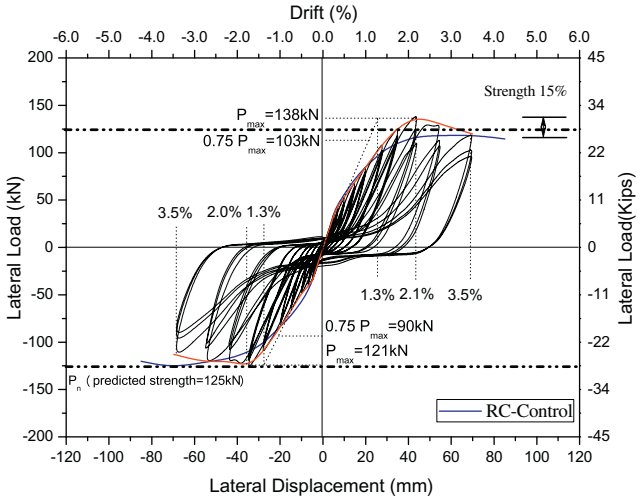

Fig. 20. Load-Drift Ratio of PC-I-25 Specimens.

measured at the loading point on the column. The nominal strength of all the specimens under positive and negative loading was measured at a drift ratio of 1.5–2%, respectively. There were no strength degradations until a drift ratio of 3.5% and the strength decrease was observed from approximately a drift ratio of 4.25%.

In the monolithic RC specimen(refer to Fig. 16), ultimate strength (119 kN) was observed at a drift ratio of 3.5% and hysteretic behavior was stable until a drift ratio of 4.25% without displaying rapid deterioration in load-carrying capacity. In case of PC-OH-50(refer to Fig. 17), the specimen with the outside type connection with in situ ECC area of 500 mm (1.4d), the ultimate strength (155 kN) was measured at a drift ratio of 3.5% and then load value dropped rapidly. It is deduced that stress concentrated in the area of the plastic hinge generated from the in situ ECC area because the area of the plastic hinge was reinforced widely. The ultimate strength (133 kN) of PC-OH-25(refer to Fig. 18), with smaller in situ ECC area was recorded at a drift ratio of 2.2% and ideal hysteretic behavior was displayed until a drift ratio of 4.25%. It was found that increasing in situ ECC area using the steel connector and the ECC to additionally reinforce the area of the beam plastic hinge improved strength by approximately 15%. PC-IH-50 showed (refer to Fig. 19), stable hysteretic behavior until a drift ratio of 4.25%. In case of PC-I-25 (refer to Fig. 20) with smaller in situ ECC area, the ultimate strength (138 kN) was obtained at a drift ratio of 2.2% and hysteretic behavior was stable until a drift ratio of 3.5%. While the maximum load-carrying capacity of the two precast specimens where the steel connectors and the ECC were used in the joint areas was higher than that of the RC specimen by 15% on average, no significant difference associated with the connection detail was found. However, the increase in in situ ECC area to extend the reinforcement of the plastic hinge area improved ductility more than load-carrying capacity (approximately 6%). It is deduced that the additional reinforcement of the plastic hinge area with in situ ECC of 250 mm (0.7d) in the outside type connection and 500 mm (1.4d) in the inside type connection is efficient to deliver the load applied to column to the joint and beams, respectively. While follow-up studies should be conducted to decide appropriate area of reinforcement, 1/8–1/4 of beam length seems to be reasonable (refer to Table 2).

5.3. Strain in steel bars

The U.S. regulation for special moment structures (PC and PSC) describes that a plastic hinge be transferred not to a joint but to the inside of beams in order for the capacity of the structures to be the same as that of monolithic beam-to-column structures. Thus, stress distribution of beam main bars installed up to the distance of 2.0d from the column surface was analyzed as shown in Fig. 21 to investigate whether stress discontinuity between the members would occur at the beam-to-column joint where the steel connector and the ECC were used to precast U-shaped sectional area or the plastic hinge would be transferred to the inside of beams as a drift ratio increased as in the case of monolithic structures.

As depicted in Fig. 21, in case of the RC specimen where shear redundancy ratio was 1.26 (joint shear strength/joint shear strength upon the flexural yield of beam. See Table 1), bending strength ratio was 1.6 and the joint was planned to fail after the yield of the main tensile bars in the beams, initial yield was observed near the joint at a drift angle of 1%, and the bars yielded one after the other as load increased. In case of the specimens with the outside type connection with shear redundancy ratio of 1.09 and bending strength ratio of 1.3, stress distribution at the steel connector inserted to the beam and strain in the steel bars were similar to those of the RC specimen. The steel bars connected to the steel plate at the distance of 2.0d from the column surface yielded before a drift ratio of 2% while they yielded after a drift ratio of 2% in the specimen with the inside type connection with shear redundancy ratio of 1.54 and bending strength ratio of 1.3 probably due to greater ductility of the members enabled by the greater redundancy ratio. In addition, smaller in situ ECC area led

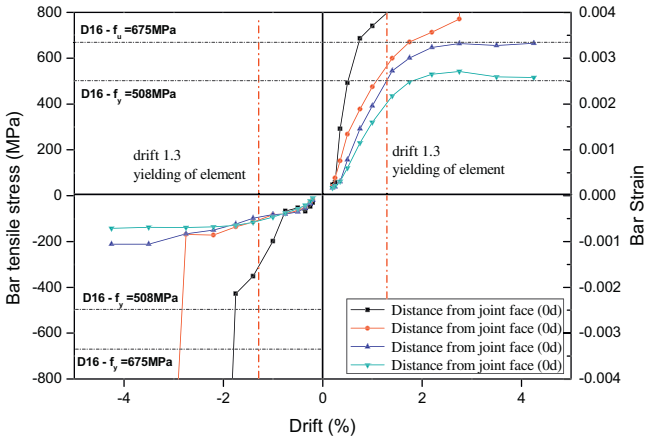

(a) RC-Control

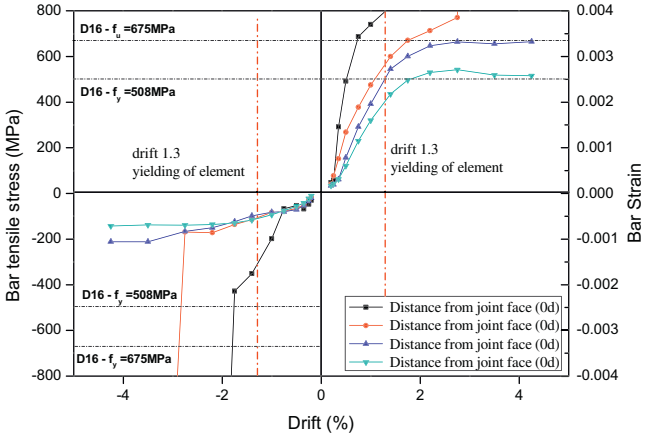

(b) PC-OH-50

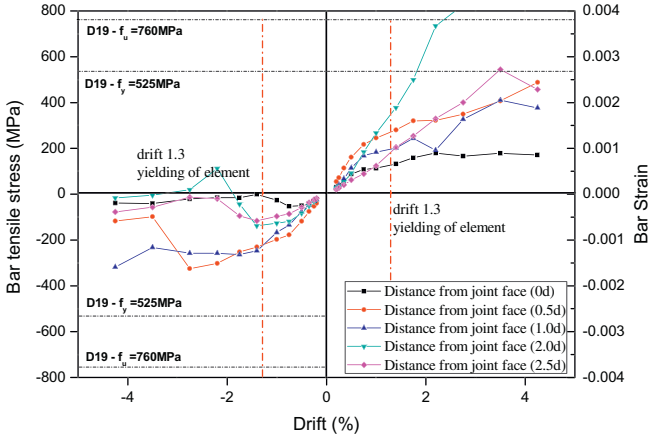

(c) PC-OH-25

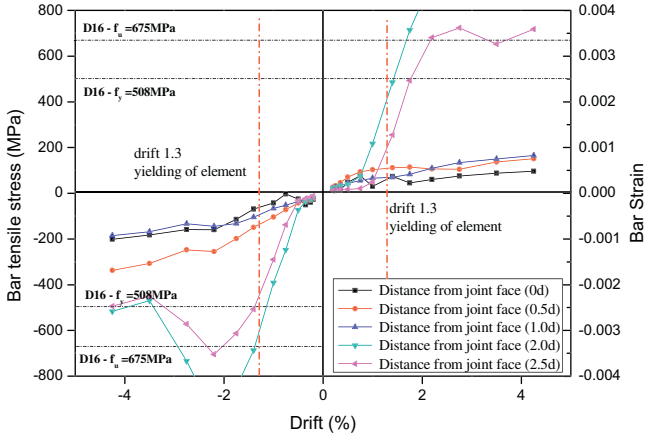

(d) PC-IH-50

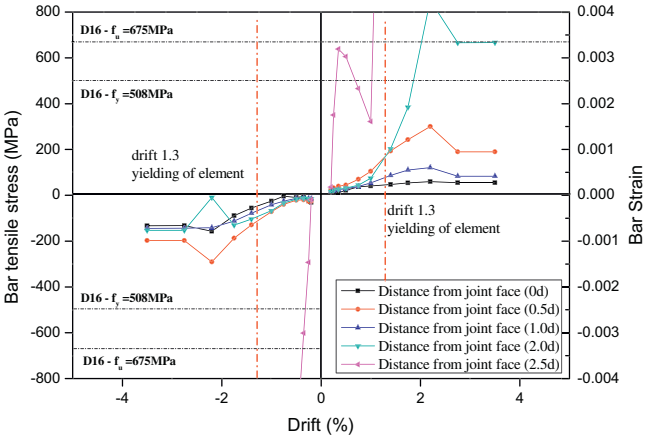

(e) PC-I-25

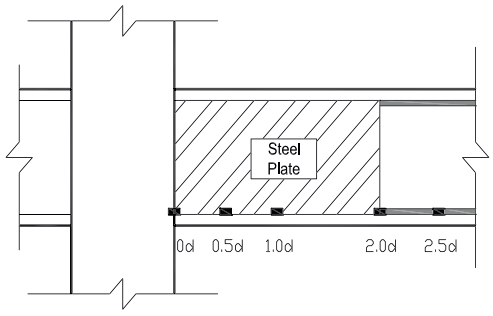

(f) W.S.G Location

Fig. 21. Stress of bottom & top reinforcement of the beam.

to the increase in the stress of the steel connectors and the bars probably because of bond stress between the ECC and concrete.

Previous studies found that shear strength of a joint improves in proportion to the increase in steel ratio of lateral steel bars inserted in the joint. Therefore, shear deformation angle of the joints and stress change of the lateral bars in the joints were analyzed for the specimens except for PC-I-25 with the smallest in situ ECC area in order to evaluate the effectiveness of the lateral bars in the connection detail suggested in this study.

As shown in Figs. 22 and 23, the stress distribution of the monolithic RC specimen was almost identical regardless of the location of the joint. It can be mentioned that the improvement in shear strength was attributable to lateral bars to some degree. However, when it comes to the three precast specimens where the ECC and the steel connectors were used in the joints, the stress change at the lateral bars was nominal probably since shear deformation angles in the precast specimens were smaller than that in the monolithic RC specimen. It was found that shear deformation at the

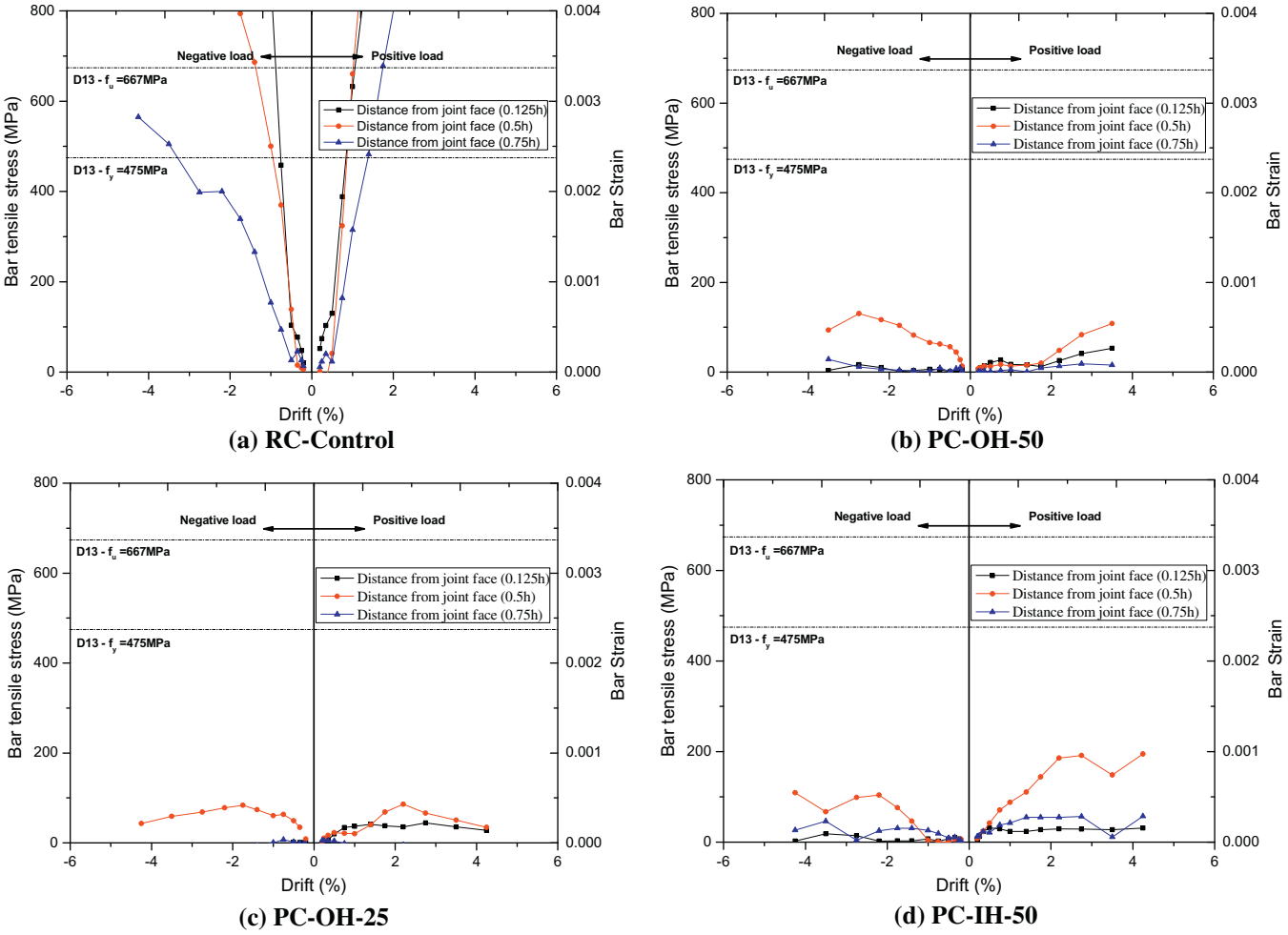

Fig. 22. Stress of joint transverse reinforcement.

joints was mitigated as the capacity of the steel connectors in the columns and the ECC in the joints improved. Accordingly, the influence of the lateral bars in the joints on the improvement in shear strength was nominal in the connection detail proposed in this study due to the influence of the ECC and the steel connectors.

6. Analysis of test results

6.1. Strength and stiffness

Table 3 provides the structural capacities of the specimens evaluated based on the ACI T1.1-01 [26]. It suggests that the strength after a drift angle of 3.5% be over 75% of the initial strength to prevent building collapse due to a severe earthquake. It was observed that the connection suggested in this study maintained over 75% of the initial strength at the last cycle when a drift ratio was 3.5%.

Fig. 24 shows the change in stiffness in the specimens, which is the presentation of stiffness change connecting maximum displacement under positive and negative loading as the ratio against initial yield stiffness. While stiffness deteriorated in all of the specimens as inelastic hysteretic cycles increased, it was greater in the specimens with the outside type connection which had relatively higher beam strength. In the specimens where members were connected at a distance, deterioration in stiffness was significant depending on in situ ECC area providing excellent ductility and was almost twice after a drift ratio of 2%. While the degree of and deterioration in stiffness in the specimens with the inside type connection were similar to those in the monolithic specimen, deterioration in stiffness in the former was more stable than in the latter after a drift ratio of 1.5%. Still, deterioration in stiffness was mitigated after a drift ratio of 1% in the specimens with the inside type connection mainly due to the strain hardening enabled by the improvement in the tensile deformability of concrete by the ECC poured inside the joints and the areas of the plastic hinge. The difference in stiffness deterioration after a drift ratio of 3.5% between the two precast specimens with the inside type connection seemed attributable to the extension of cracks at the joint of PC-I-25 specimen without lateral reinforcement. If stiffness deteriorates significantly after a severe earthquake, even small load can cause great deformation to the structure and make it unstable. Therefore, the ACI prescribes that the stiffness in the 3rd cycle at a drift ratio of 3.5% be greater than 5% of the initial stiffness. As shown in Table 3, all of the three specimens met the requirement (see Fig. 25).

Displacement ductility, one of the criteria of nonlinear behavior of structures subjected to seismic loading, is defined as the ratio of displacement at the maximum load to displacement at the yield load as expressed by Eq. (3) and the results are provided in Table 2

$$\mu = \frac{\delta_{\max}}{\delta_y} \tag{3}$$

where $\delta_{\max}$ and δ_y = displacement at the maximum and the yield load, respectively. The displacement at the yield load of the specimen was first computed using both well-known Park and Offset methods and then the displacement value using Park method was

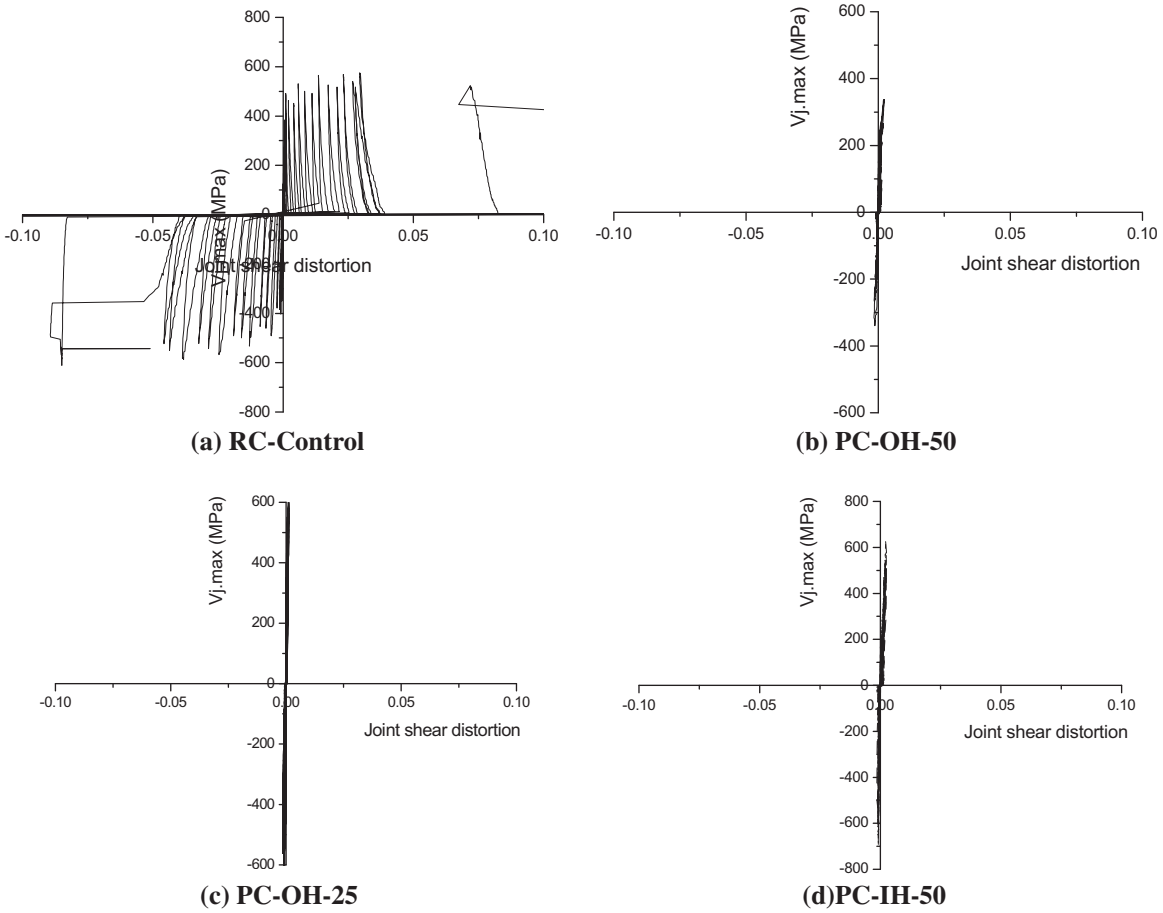

Fig. 23. Joint shear distortion relations.

chosen since the value from Park method was similar to the one when main reinforcement in the beam yielded. As summarized in Table 2, the displacement ductility of the PC specimens was equivalent to that of the RC control specimen constructed with all-in-one concrete, which means that the PC specimens are reliable from the standpoint of ductility even though the PC specimens have smaller flexural strength ratio than the RC specimen. Furthermore, the outside type specimen showed relatively better ductility than the inside type specimen. This was mainly due to the difference of strengthening capacity caused by the strain hardening phenomenon of the ECC which is fiber-reinforced concrete.

6.2. Energy dissipation

Ductile behavior of a structure upon an earthquake is closely related to energy dissipation. In other words, greater energy dissipation improves seismic performance. (refer to Fig. 25) Fig. 26 shows energy dissipation index [29] obtained by dividing energy

Table 3
Comparison between test results and ACI T1.1-01 accept criteria.

Specimen			During 3.5% and 4.25% drift cycle			
Acceptance criteria			P_{3rd}/P_{max} ⩾0.75	β ⩾0.125	K_{re}/K ⩾0.05	K_{un}/K' ⩾0.05
RC-control	drift 3.5%	Pos	0.87	0.19	0.5	0.4
		Neg	0.83			
	drift 4.25%	Pos	0.75	0.18	0.19	0.17
		Neg	0.70			
PC-OH-50	drift 3.5%	Pos	0.70	0.30	0.30	0.37
		Neg	0.77			
PC-OH-25	drift 3.5%	Pos	0.75	0.30	0.32	0.51
		Neg	0.88			
	drift 4.25%	Pos	0.54	0.30	0.21	0.11
		Neg	0.59			
PC-IH-50	drift 3.5%	Pos	0.78	0.20	0.11	0.15
		Neg	0.75			
	drift 4.25%	Pos	0.35	0.19	0.06	0.09
		Neg	0.34			
PC-I-25	drift 3.5%	Pos	0.75	0.24	0.49	0.14
		Neg	0.76			

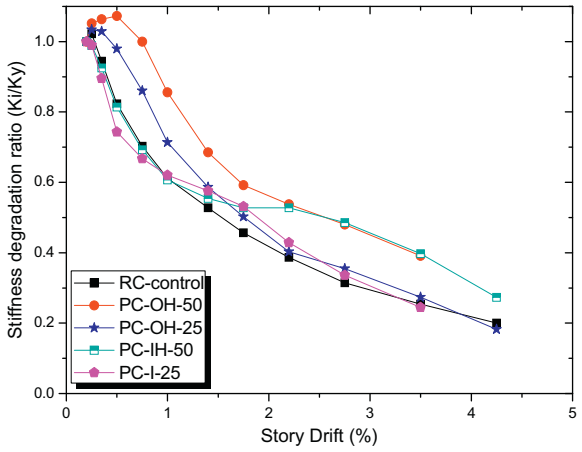

Fig. 24. Stiffness degradation.

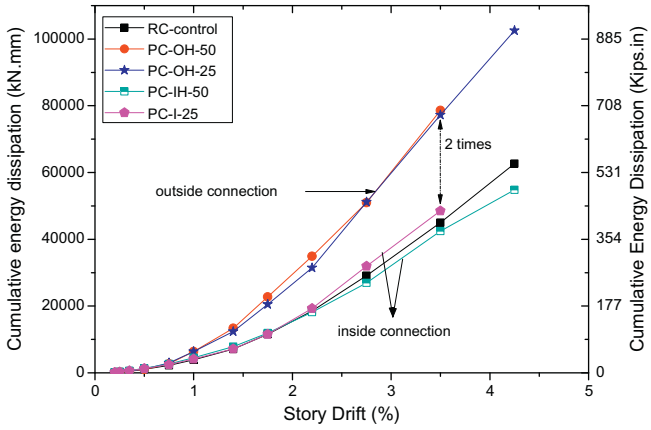

Fig. 25. Energy dissipation.

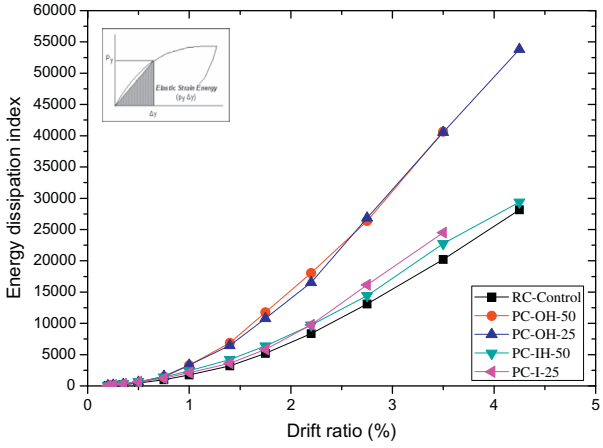

Fig. 26. Energy dissipation index.

dissipation at yield into cumulative energy dissipation and energy dissipation in each cycle.

At drift ratio of 3.5%, while cumulative energy dissipation was greater in precast specimens with outside type connection than in monolithic RC specimen by approximately 42%, the difference between precast specimens with inside type connection and RC specimen was merely about 6%. However, PC-IH-50 specimen which had lateral bars in joint and larger in situ ECC area showed low energy dissipation seemingly because pinching resulting from relatively greater damage to plastic hinge area at beam degraded energy dissipation.

The ACT requires that energy dissipation ratio be over 1/8 (=0.125) in the 3rd cycle at drift ratio of 3.5% to secure stable energy dissipation for structures. As shown in table 3, all of the specimens satisfied the requirement at drift ratio of 3.5% and 4.25%.

7. Conclusions

The conclusion of the cyclic load test conducted for the half-scale specimens to identify structural characteristics of the precast beam-to-column connection detail using the steel connectors and the ECC can be drawn:

(1) All the specimens showed the typical flexural failure mode and the precast beam–column connections behaved monolithically until failure.
(2) Stress discontinuity between the members associated with the steel connectors and the ECC was not observed and the load was effectively transferred to the beam and joint.
(3) The maximum strength of the specimens with the inside and the outside type connections was improved by 15% when compared with the control specimen and the specimens with the outside type connection showed greater strength and energy dissipation than those with the inside type connection. The extended reinforcement of the plastic hinge area in the beams improved strength by approximately 15%. Therefore, it can be concluded that 250 mm ($0.7d$) is enough to deliver the load applied to the columns to the joints and beams. While further research is needed, 1/8–1/4 of beam length is considered to be appropriate.
(4) In terms of shear strength of the joint, the result of the test in this study corresponded to the finding of the previous study that the capacity of lateral bars is improved as that of the joints improves. However, although the influence of lateral bars on strength improvement was nominal due to the improvement in confinement effect enabled by the ECC and the steel connectors, they are still necessary to control cracks at the joints; and
(5) The connection detail developed and suggested in this study which have elastic joint and steel plate connector satisfied the requirement prescribed in the ACI structural guideline and thus was verified to provide excellent seismic performance. So elastic joint with bolted assembly with steel plate type connection can be suggested for the design of precast concrete buildings in seismic area.

Acknowledgments

This research was supported by NRF of Korea (2013R1A1A2010717, ERC) and grant(Code 11-Technology Standardization-07-01) from R&D Policy Infra Program funded by Ministry of Land, Transportation and Maritime Affairs(MLTM) of Korean government.

References

[1] Restrepo JI, Robert P, Buchanan AH. Tests on connections of earthquake resisting precast reinforced concrete perimeter frames of buildings. PCI J 1995;40(4):44–61.
[2] Alcocer SM, Carranza R, Perez-Navaratte D, Martinez R. Seismic tests of beam to column connections in a precast concrete frame. PCI J 2002;47(3). p. 70–89.
[3] Kim TH, Lee HM, Kim YJ, Shin HM. Performance assessment of precast concrete segmental bridge columns with a shear resistant connecting structure. J Eng Struct 2010;32(5):1292–303.
[4] Blandon JJ, Rodriguez ME. Behavior of connections and floor diaphragms in seismic-resisting precast concrete buildings. PCI J 2005;50(2):56–75.

[5] Park R. A perspective on the seismic design of precast concrete structures in New Zealand. PCI J 1995;40(3):40–60.
[6] Ghosh SK, Nakaki SD, Krishnan K. Precast structures in regions of high seismicity: 1997 UBC design provisions. PCI J 1997;42(6):76–93.
[7] Nakaki SD, Stanton JF, Sritharan S. An overview of the PRESSS five-story precast test building. PCI J 1999;44(2):26–39.
[8] Priestley MJN, MacRae GA. Seismic tests of precast beam-to-column joint subassemblages with unbonded tendons. PCI J 1996;41(1). p. 64–81.
[9] Restrepo JI, Park R, Buchanan AH. Design of connections of earthquake resisting precast reinforced concrete perimeter frames. PCI J 1995;40(5): 68–80.
[10] Gustavo JPM, Prabuddha D, Subhash CG. Development of connections between hybrid steel truss–FRC beams and RC columns for precast earthquake-resistant framed construction. J Eng Struct 2005;27(13):1931–41.
[11] ACI-ASCE Committee 352. Recommendations for design of beam_column connections in monolithic reinforced concrete structures (ACI 352R–02). ACI; 2002. p. 37.
[12] ACI 318M-05. Building code requirements for structural concrete and commentary. Michigan(USA): American Concrete Institute(ACI), Committe, vol. 318; 2005. p. 299–334.
[13] Englekirk RE. Overview of PCI workshop on effective use of precast concrete for seismic resistance. PCI J 1986;31(6):48–58.
[14] Priestley MJN. Research needs for precast seismic structural system. Structural systems research report. San Diego: University of California; 1988. Report No. 88(06).
[15] Englekirk RE. Development and testing of a ductile connector for assembling precast concrete beams and columns. PCI J 1995;39(2):36–51.
[16] Stanton JF, Hawkins NM, Hicks TR. PRESSS Project 1.3: connection classification and evaluation. PCI J 1991;36(5):62–71.
[17] Priestley MJN. The PRESSS Program—current status and proposed plans for Phase III. PCI J 1996;41(2):22–40.
[18] Soubra KS, Wight J14K, Naaman AE. Cyclic response of fibrous cast-in-place connections in precast beam-column subassemblages. ACI Struct J 1993;90(3): 316–23.
[19] Khaloo AR, Parastesh H. Cyclic loading of ductile precast concrete beam–column connection. ACI Struct J 2003:440–5. May–June.
[20] Fischer G, Li V. Influence of matrix ductility on tension-stiffening behavior of steel reinforced engineered cementitious composites (ECC). ACI Struct J 1993; 99(1):104–11.
[21] Li V, Leung C. Steady-state and multiple cracking of short random fiber composite. J Eng Mech 1992;118(11):2246–64.
[22] Bahjat AA, Wight GK. Experimental study of moving beam plastic hinging zones for earthquake design of RC building. department of civil engineering. The University of Michigan 1985. Report No. 85(11).
[23] Al-Haddad MS, Wight JK. Relocating beam plastic hinging zones for earthquake resisting design of reinforced concrete buildings. ACI Struct J 1988; 85(2):123–33.
[24] Bracci JM, Dooley KL. Effect of column-to-beam strength ratio on seismic performance of rc moment frames. Texas A&M University. Technical Report No. CBDC 01-02; 2001.
[25] Kuntz GL, Browning J. Reduction of column yielding during earthquakes for reinforced concrete frame. ACI Struct J 2003;100–S59(September–October): 573–80.
[26] Lee H. Revised rule for concept of strong-column weak-girder design. J Struct Eng 1996;122(4):359–64.
[27] Lee JY, Kim JY, Oh GJ. Strength deterioration of reinforced concrete beam-column joints subjected to cyclic loading. J Eng Struct 2009;31(9):2070–85.
[28] ACI T1.1R-01. Commentary on acceptance criteria for moment frames based on structural testing. ACI Manual of Concrete Practice; 2002. p. 1–7.
[29] Darwin D, Nmai CK. Energy dissipation in RC beams under cyclic load. J Struct Eng, ASCE 1986;112(8):1829–46.